

Resonance signals in pion-nucleon scattering from speed plots and time-delay

R.L. Workman and R.A. Arndt

Center for Nuclear Studies, Department of Physics

The George Washington University, Washington, D.C. 20052

(Dated: November 1, 2018)

Abstract

We compare a number of methods used to locate resonances. These include the speed plot, the time-delay method of Eisenbud and Wigner, the time-delay matrix of Smith, and a modification proposed by Ohmura. Numerical results show a consistency not previously reported. One time-delay method gives the most consistent results, supporting the conclusions of a recent theoretical study.

PACS numbers: PACS numbers: 11.55.Bq, 11.80.Et, 11.80.Gw

Given a set of elastic scattering amplitudes or, for a multi-channel process, the full S-matrix, the most direct way to locate resonances involves a search for poles in the complex energy plane. To do this, one must have an analytic representation that can be continued, correctly accounting for the branch cuts. If only numerical values of the amplitudes are available, less sophisticated methods may still be applied, at least for those resonances with a clear resonance signature.

Here we will compare two such methods – the speed-plot, advocated by Höhler [1], and the time-delay, which was first studied for elastic and multi-channel scattering by Eisenbud and Wigner [2, 3]. These methods have recently been examined in terms of their theoretical basis [4, 5]. Here we will briefly review the proposed methods and make comparisons based on their ability to correlate speed or time-delay peaks with resonance energies. In doing so, we will gain a better understanding of some puzzling results associated with previous applications of these methods. One particular time-delay method is advocated in the recent study of Ref. [5]. A comparison of our numerical results appears to support their conclusions.

In 1948, Eisenbud [2] proposed a method for locating resonances, in both single- and multi-channel scattering, based on the time-delay associated with a wavepacket. Wigner quoted [3] a time-delay result in a later paper focused on the restrictions of causality. The result of Eisenbud was

$$\Delta t^E = \hbar \frac{d}{dE} [\arg(S - 1)], \quad (1)$$

which for a single channel, gives the result

$$\Delta t^E = \hbar \frac{d\delta}{dE}, \quad (2)$$

δ being the phase shift. The result quoted by Wigner was larger by a factor of 2. A reason for this factor was later noted by Wigner in Ref. [6, 7].

Smith [8] derived a time-delay matrix, based on the flux passing through an interaction region of radius R . His result for the average lifetime of a metastable state due to a collision beginning in the i^{th} channel was

$$Q = -i\hbar \frac{dS}{dE} S^\dagger, \quad (3)$$

S being the S-matrix including all open channels. Smith then claimed that his result could be connected to the Eisenbud result, using the following representation

$$\Delta t_{ij}^S = \text{Re} \left[-i\hbar (S_{ij})^{-1} \frac{dS_{ij}}{dE} \right], \quad (4)$$

implicitly attributed to Eisenbud. From the above two results, Smith noted that

$$Q = \sum_j S_{ij}^* S_{ij} \Delta t_{ij}^S, \quad (5)$$

followed trivially. Notice, however, that Eqs. (1) and (4) are *not* equivalent.

Objections to Smith's time-delay formalism were expressed in the extensive study of Ohmura [9] as noted in Ref. [6]. Ohmura's result agreed with that of Eisenbud, though this was not apparent as the Eisenbud thesis remained unpublished and the Eisenbud result was misquoted by Smith. Ohmura further claimed that Smith's results could be made more consistent by subtracting off a term due to the outgoing unscattered wave, giving for the average time delay [9] of a wavepacket beginning in the i^{th} channel

$$\langle \Delta t_i \rangle_{Av} = N_{ii}^{-1} \text{Re} \left[-i\hbar \sum_n (S_{in}^* - \delta_{in}) \frac{dS_{jn}}{dE} \right], \quad (6)$$

with

$$N_{ii} = \sum_j (S_{ij}^* - \delta_{ij})(S_{ij} - \delta_{ij}). \quad (7)$$

Ohmura's result can be found if one starts with the expression

$$2iT^*T \frac{d}{dE} \{\arg T\} = T^* \frac{dT}{dE} - T \frac{dT^*}{dE}, \quad (8)$$

uses Eq. 1, and multiplies by appropriate factors of \hbar and $2i$, to obtain

$$\Delta t_{ij}^E S_{ij} S_{ij}^* = \text{Re} \left[-i\hbar S_{ij}^* \frac{dS_{ij}}{dE} \right], \quad (9)$$

for $i \neq j$. This can be compared to Smith's result in Eq. 5. The sum differs in the $i = j$ term, which is constructed to be consistent with Eq. 1, in the single-channel scattering limit, rather than Eq. 4. However, this sum is not a proper average, since the weights do not add to unity. To have the sum represent the average of Eisenbud time-delays, the weights must be renormalized, and the factor N_{ii} in Eq. 7 is added for this purpose.

In the following numerical comparison, we will be using the partial-wave decomposed S-matrix. However, the results of Eisenbud were derived assuming a single dominant partial wave, whereas the Ohmura result was based on the use of the full S-matrix [5, 9]. It is thus surprising how well these methods work, applied to a set of partial wave amplitudes derived from a fit to data.

In Figs. 1 and 2, we compare these time-delay methods, and the more common speed-plot method, applied to amplitudes obtained in a fit to elastic pion-nucleon scattering. Figure 1

compares the time delay results of Smith and Ohmura, based on the scattering S-matrix. In the fit to pion nucleon elastic scattering and ηN production data of Ref. [10], a multi-channel Chew-Mandelstam K-matrix formalism was used. This produced a multi-channel S-matrix, with each channel having the required poles and cuts (for ηN , $\pi\Delta$ and ρN). As the $\pi\Delta$ and ρN channels were constrained only by the πN channel inelasticity, the displayed results are a test of the method and would be improved using a more detailed multi-channel analysis.

Figure 1(a) shows the S_{11} channel, containing the N(1535) and N(1650) resonances, plus a cusp at the ηN threshold. Peaking in the time delay is evident at both resonances, denoted by arrows at the real parts of the pole positions [11]. Separation of the N(1535) and the threshold cusp is clear using both forms. In Figure 1(b), results for the P_{11} (Roper) channel are given. Finally, in Figure 1(c), the D_{13} resonance is shown. In these plots, the normalization factor N_{ii} is proportional to the imaginary part of the πN elastic T-matrix. For the Roper resonance in particular, dropping this factor causes a significant shift in the peak position, as the imaginary part of $T_{\pi N}$ is rapidly increasing above and below the energy corresponding to the real part of the pole position.

In Figure 2, we display the speed plot, which is given by the absolute value of dT/dW , and compare this to the single-channel result of Eisenbud, which is given by the energy derivative of the phase of the T-matrix. Again, for orientation, we locate the real parts of the associated pole positions. Peaks in the speed plots again correspond to the pole positions and the Eisenbud time-delay peaks. Separation of the ηN cusp and N(1535) resonance is still evident, though not as clear as in Figure 1. (The region of negative time-delay between the resonances is not plotted.) In the study of Höhler, the ηN threshold and N(1535) resonance signal were combined into a single peak at the ηN threshold. The separation is visible in our case only if a very fine grid of energies is used.

All methods agree when applied to the elastic P_{33} partial wave and the $\Delta(1232)$ resonance. All methods find a peak corresponding to the pole position. We have also applied these methods to the higher partial waves and generally find peaks for all PDG 4-star resonances using either the S-matrix methods of Smith and Ohmura or the single-channel results obtained using the Eisenbud time-delay or speed plot. These results are quite different from those of Ref. [12], finding no prominent peaks for most of the isospin 3/2 resonances. In that work Eq. 4 was used for both elastic and inelastic resonances.

Problems with resonance location and the use of Eq. 4 are clearly illustrated if we examine

the 4-star $\Delta(1950)$ resonance, which produces a nearly canonical resonance loop in the Argand plane. This resonance has $\Gamma_{\pi N}/\Gamma_T < 1/2$ and therefore the loop passes below the center of the Argand circle. The four methods applied in Figs. 1 and 2 are compared to Eq. 4 in Fig. 3. All produce peaks at the same point, the real part of the energy associated with the pole, except Eq. 4, which produces a sharp dip closer to resonance mass found in a Breit-Wigner fit to the amplitude. In Figs. 4 and 5 of Ref. [12], resonance positions were associated with the positive time-delay shoulder, which is also evident in Fig. 3, prior to the time-advance spike.

One 4-star resonance, the $\Delta(1620)$ occurring in the S_{31} partial wave, breaks the pattern described above. The amplitude, time-delay, and speed plots for this partial wave are displayed in Fig. 4. In an Argand diagram, this amplitude first moves in a clockwise direction before beginning the (anti-clockwise) resonance loop. Both matrix methods and the speed plot produce peaks near the resonance energy. However, the Ohmura result is shifted from the pole position. Both of the single-channel time-delay results fail to peak at the resonance.

In summary, we have examined a number of candidate methods for the location of resonances using either the T-matrix for a single channel, or the S-matrix accounting for all open channels. These methods generally produce a peak at an energy associated with the real part of the pole position and show remarkable agreement in most cases. One method which has been used extensively, based on the energy derivative of the channel phase shift, does not correlate with the pole position, producing a peak at the pole mass of the $\Delta(1232)$, but time-advance dips near the Breit-Wigner masses of some other more inelastic resonances. The $\Delta(1620)$ resonance appears to provide the most demanding test (from a well established state). For this state, the matrix methods and speed plot peak near the resonance energy, the single-channel time-delay methods do not. Apart from the speed plot, only the S-matrix method of Smith appears to consistently correlate with resonance pole positions. This agrees with a recent claim from Kelkar and Nowakowski [5] who have reviewed the theoretical basis for the methods used in the present numerical study. We expect these result will motivate further investigations parallel to those reported in Ref. [4].

Acknowledgments

We thank N. Kelkar for pointing out the relevance of her recent work on this topic. This work was supported in part by the U.S. Department of Energy Grant DE-FG02-99ER41110 and funding provided by Jefferson Lab.

-
- [1] G. Höhler and A. Shulte, πN Newsletter 7, 94 (1992): ISSN 0942-4148.
- [2] L. Eisenbud, Ph.D. thesis, Princeton University, 1948 (unpublished).
- [3] E.P. Wigner, Phys. Rev. **98**, 145 (1955).
- [4] 'Extraction of resonances from meson-nucleon reaction', N. Suzuki, T. Sato, and T.S.H. Lee, arXiv:0806.2043 [nucl-th].
- [5] 'Analysis of averaged multichannel delay times', N.G. Kelkar, M. Nowakowski, arXiv:0805.0608 [nucl-th].
- [6] F. Goldrich and E.P. Wigner, in *Magic Without Magic: John Archibald Wheeler*, W.H. Freeman, San Francisco, 1972, p.159.
- [7] This factor of 2 was also noted in H. Habertzettl and R. Workman, Phys. Rev. C **76**, 058201 (2007).
- [8] F.T. Smith, Phys. Rev. **118**, 349 (1960).
- [9] T. Ohmura, Prog. Theor. Phys. Suppl. **29**, 108 (1964).
- [10] R.A. Arndt, W.J. Briscoe, I.I. Strakovsky, and R.L. Workman, Phys. Rev. C **74**, 045205 (2006).
- [11] Pole positions were determined by extrapolating the analytic expression for each partial-wave amplitude into the complex energy plane.
- [12] N.G. Kelkar, M. Nowakowski, K.P. Khemchandani, S.R. Jain, Nucl. Phys. A730, 121 (2004).

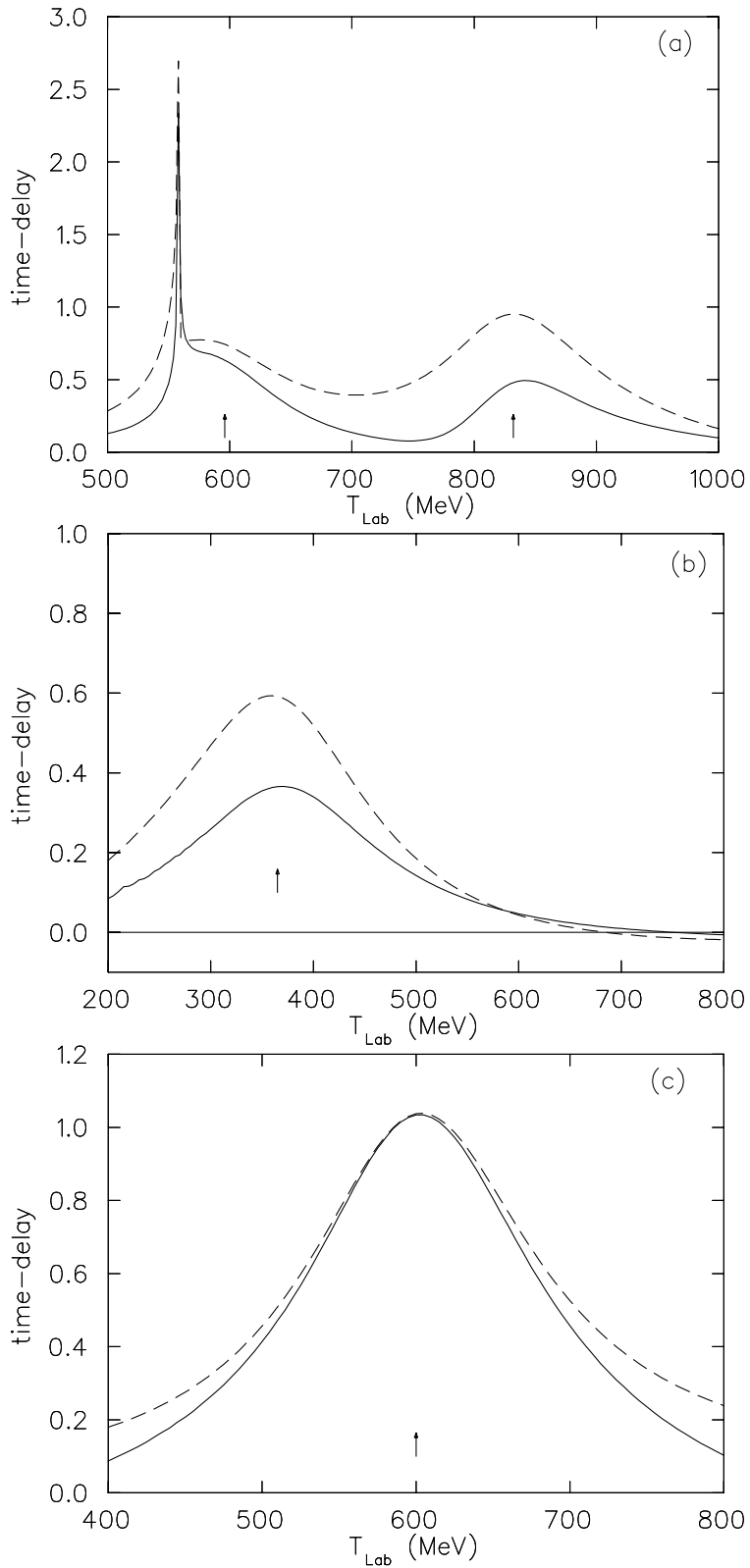


FIG. 1: Time-delay plots based on the S-matrix approaches of Smith [8] (dashed) and Ohmura [9] (solid) in arbitrary units. Arrows denote the real part of resonance pole positions for (a) the S_{11} , (b) P_{11} , and (c) D_{13} partial waves (see text).

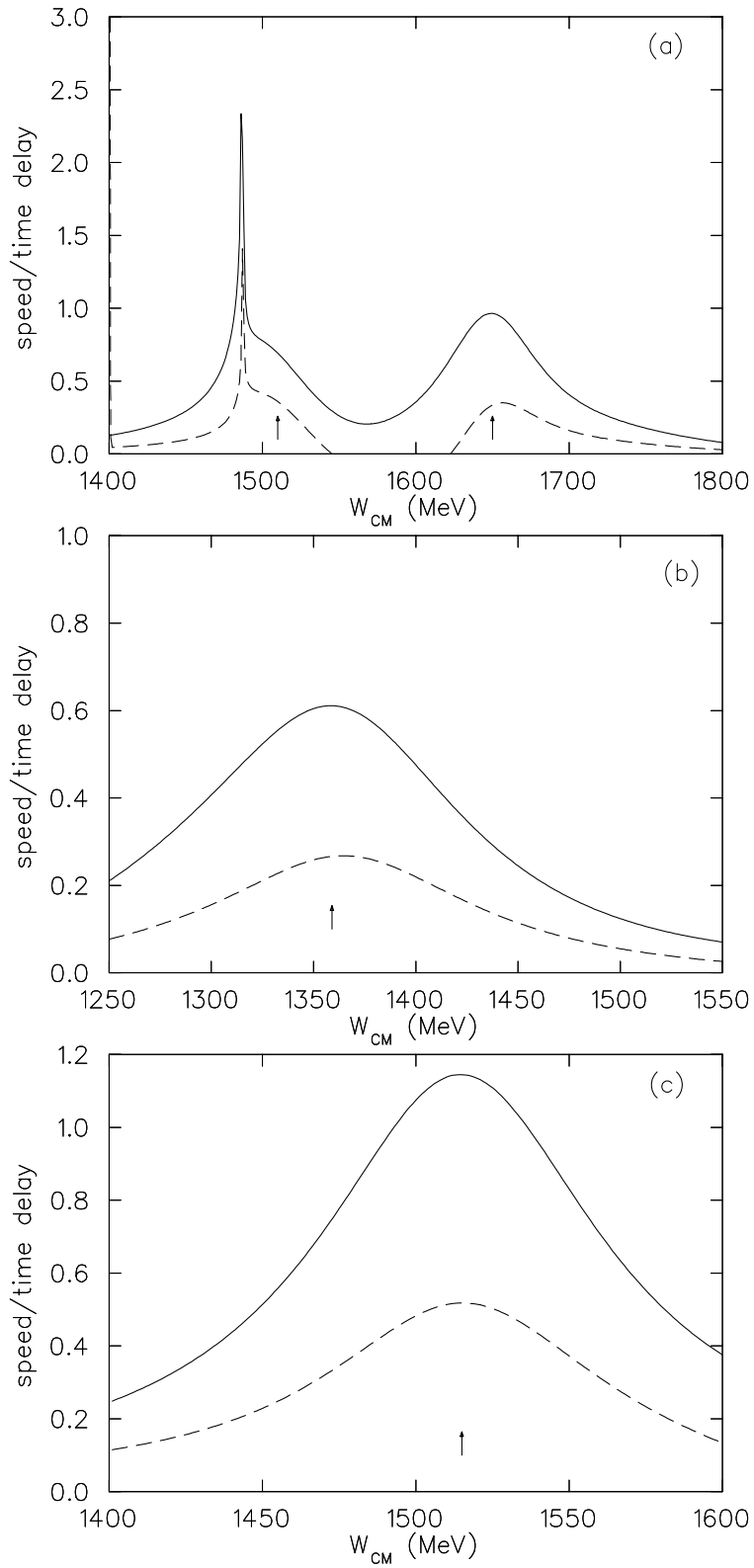


FIG. 2: Speed plots (solid) and Eisenbud single-channel time-delays (dashed) in arbitrary units. Arrows denote real parts of resonance pole positions for (a) the S_{11} , (b) P_{11} , and (c) D_{13} partial waves (see text).

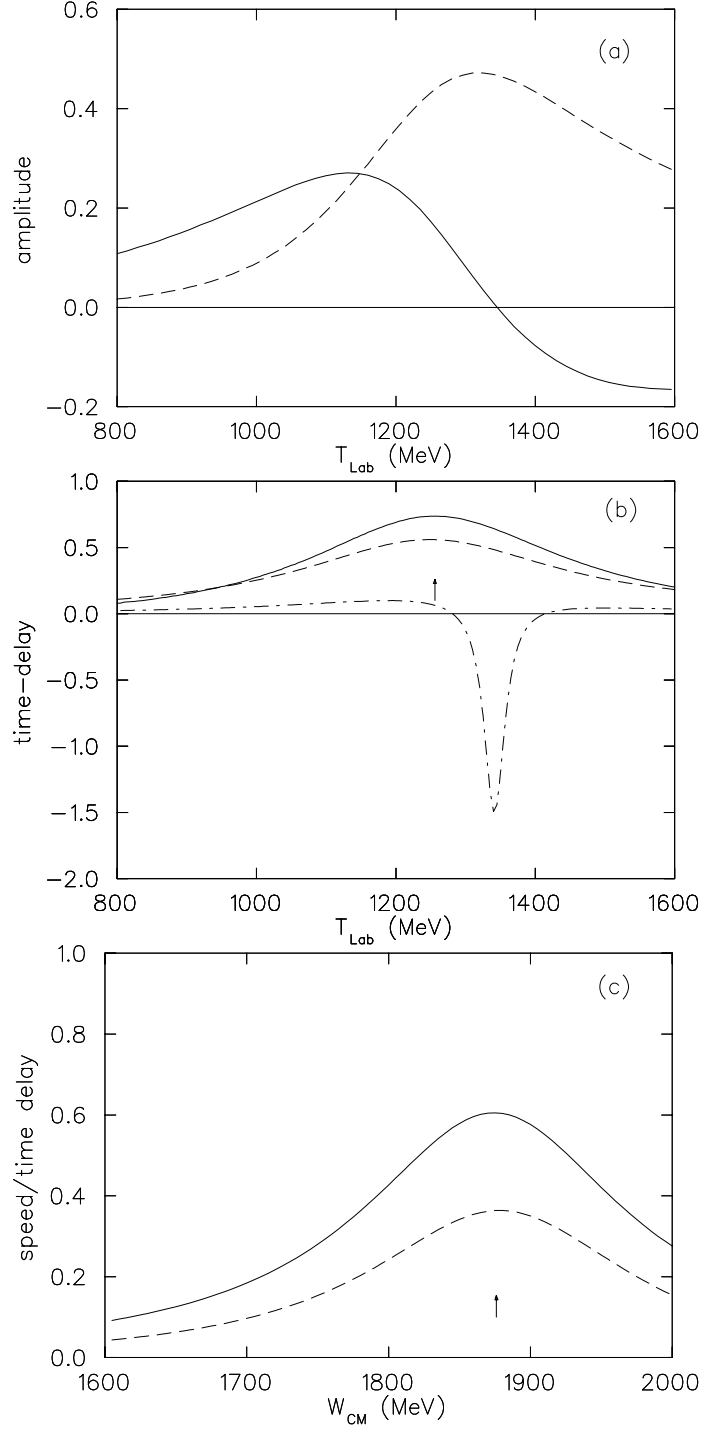


FIG. 3: Time-delay and speed plots for the $F_{37} \pi N$ resonance $\Delta(1950)$ in arbitrary units. Arrows denote the real part of resonance pole position. Plotted are (a) the real(solid) and imaginary(dashed) parts of the dimensionless $F_{37} \pi N$ amplitude, (b) the matrix average time delay of Smith (dashed) and Ohmura (solid), the result using Eq. 4 (dot-dashed), (c) the Eisenbud single-channel time delay (dashed) and the speed (solid).

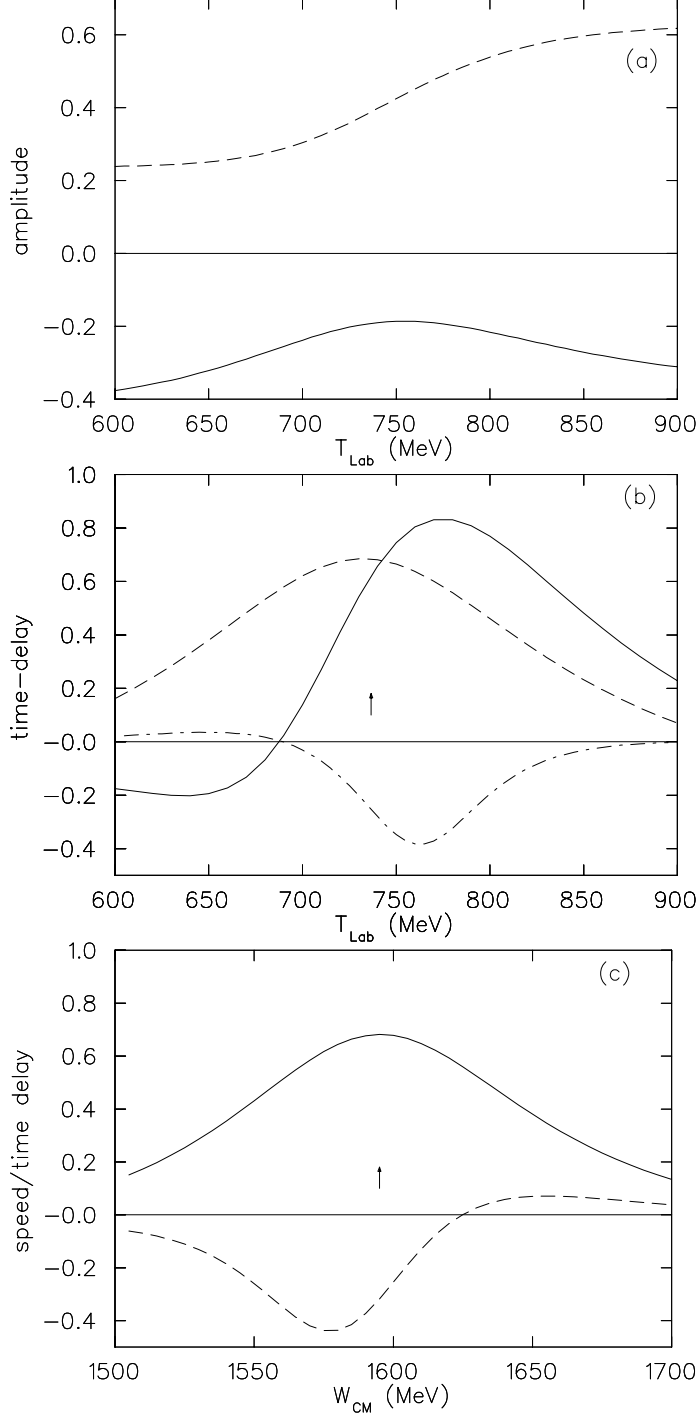


FIG. 4: Time-delay and speed plots for the S_{31} πN resonance $\Delta(1620)$ in arbitrary units. Arrows denote the real part of resonance pole position. Plotted are (a) the real(solid) and imaginary(dashed) parts of the dimensionless S_{31} πN amplitude, (b) the matrix average time delay of Smith (dashed) and Ohmura (solid), the result using Eq. 4 (dot-dashed), (c) the Eisenbud single-channel time delay (dashed) and the speed (solid).